

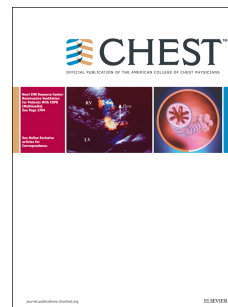
Title	CORK study in cystic fibrosis: sustained improvements in ultra-low-dose chest CT scores after CFTR modulation with ivacaftor
Authors	Ronan, Nicola J.;Einarsson, Gisli G.;Twomey, Maria;Mooney, Denver;Mullane, David;NiChroinin, Muireann;O'Callaghan, Grace;Shanahan, Fergus;Murphy, Desmond M.;O'Connor, Owen J.;Shortt, Cathy A.;Tunney, Michael M.;Eustace, Joseph A.;Maher, Michael M.;Elborn, J. Stuart;Plant, Barry J.
Publication date	2017-10-14
Original Citation	Ronan, N. J., Einarsson, G. G., Twomey, M., Mooney, D., Mullane, D., NiChroinin, M., O'Callaghan, G., Shanahan, F., Murphy, D. M., O'Connor, O. J., Shortt, C. A., Tunney, M. M., Eustace, J. A., Maher, M. M., Elborn, J. S. and Plant, B. J. (2017) 'CORK study in cystic fibrosis: sustained improvements in ultra-low-dose chest CT scores after CFTR modulation with ivacaftor', Chest, 153(2), pp. 395-403. doi: 10.1016/j.chest.2017.10.005.
Type of publication	Article (peer-reviewed)
Link to publisher's version	10.1016/j.chest.2017.10.005
Rights	© 2017, American College of Chest Physicians. Published by Elsevier Inc. All rights reserved. This manuscript version is made available under the CC BY-NC-ND 4.0 license. - http://creativecommons.org/licenses/by-nc-nd/4.0/
Download date	2024-04-18 05:46:35
Item downloaded from	https://hdl.handle.net/10468/5056



UCC

University College Cork, Ireland
Coláiste na hOllscoile Corcaigh

Accepted Manuscript



CORK study in CF: Sustained improvements in ultra-low dose chest CT scores post CFTR modulation with ivacaftor.

Nicola J. Ronan, MB BCh, Gisli G. Einarsson, PhD, Maria Twomey, Denver Mooney, David Mullane, MD, Muireann NiChroinin, MD, Grace O'Callaghan, PhD, Fergus Shanahan, Desmond M. Murphy, PhD, Owen J. O'Connor, Cathy A. Shortt, BSc, Michael M. Tunney, PhD, Joseph A. Eustace, MD, Michael M. Maher, MD, J Stuart Elborn, MD, Barry J. Plant, MD

PII: S0012-3692(17)32896-9

DOI: [10.1016/j.chest.2017.10.005](https://doi.org/10.1016/j.chest.2017.10.005)

Reference: CHEST 1385

To appear in: *CHEST*

Received Date: 23 July 2017

Revised Date: 16 September 2017

Accepted Date: 2 October 2017

Please cite this article as: Ronan NJ, Einarsson GG, Twomey M, Mooney D, Mullane D, NiChroinin M, O'Callaghan G, Shanahan F, Murphy DM, O'Connor OJ, Shortt CA, Tunney MM, Eustace JA, Maher MM, Elborn JS, Plant BJ, CORK study in CF: Sustained improvements in ultra-low dose chest CT scores post CFTR modulation with ivacaftor., *CHEST* (2017), doi: 10.1016/j.chest.2017.10.005.

This is a PDF file of an unedited manuscript that has been accepted for publication. As a service to our customers we are providing this early version of the manuscript. The manuscript will undergo copyediting, typesetting, and review of the resulting proof before it is published in its final form. Please note that during the production process errors may be discovered which could affect the content, and all legal disclaimers that apply to the journal pertain.

Title: CORK study in CF: Sustained improvements in ultra-low dose chest CT scores post CFTR modulation with ivacaftor.

Running Title: CORK study

Authors: Nicola J Ronan^{1,2} MB BCh, Gisli G Einarsson³ PhD, Maria Twomey⁴, Denver Mooney³, David Mullane¹ MD, Muireann NiChroinin¹ MD, Grace O’Callaghan^{1,2} PhD, Fergus Shanahan⁵, Desmond M Murphy^{1,2} PhD, Owen J O’Connor⁴, Cathy A Shortt¹ BSc, Michael M Tunney³ PhD, Joseph A Eustace² MD, Michael M Maher⁴ MD, J Stuart Elborn^{3,6} MD, Barry J Plant^{1,2} MD

¹Cork Cystic Fibrosis Centre, Cork University Hospital, University College Cork, Ireland

²HRB Clinical Research Facility, University College Cork, Cork, Ireland

³CF & Airways Microbiology Research Group, Queen’s University Belfast, Belfast, United Kingdom

⁴Department of Radiology, Cork University Hospital, University College Cork, Cork, Ireland.

⁵Department of Medicine, Cork University Hospital, Wilton, Cork, Ireland

⁶ Imperial College and Royal Brompton Hospital, London, UK

Corresponding Author: Barry J Plant, Cork Cystic Fibrosis Centre, Cork University Hospital University College Cork, Wilton, Cork. Email: b.plant@ucc.ie.

Contribution: NJR, FS, JAE, MMM and BJP contributed to study design. NJR, GGE, MT DM, DM, MC, GOC, DMM, OJOC, CAS, MMT, JAE, MMM, JSE and BJP contributed to data acquisition, analysis and interpretation. All authors contributed to drafting the work and final approval.

Word count: 2,493

Key Words: Cystic Fibrosis, ivacaftor, G551D, low-dose chest CT

Funding: We would like to acknowledge funding from the European Commission for CFMATTERS, Grant agreement 603038

IRB statement: Ethical approval was received from the clinical research ethics committee of the Cork Teaching Hospitals (CREC). ECM 4 (j) 02/07/13

Conflicts of interest: NJR, GGE, MT, DM, MNC, GOC, FS, CS, JAE report no conflicts of interest. Prof Elborn reports grants, personal fees and other from Vertex, personal fees and other from Galapagos, personal fees and other from Proteostasis, personal fees and other from ProQr, other from Flatley. Dr O’Connor and Prof Maher reports other from GE Healthcare, outside the submitted work. Prof Plant has received honoraria/speakers fees from Gilead Sciences, Novartis Pharmaceutical, Vertex Pharmaceutical, outside the submitted work. Dr. Mullane reports personal fees from Vertex pharmaceuticals, outside the submitted work. Dr. Murphy reports an APC grant from University College Cork and funding from the Wilton Respiratory Research Fund to support this research. He is the past recipient of an ERS fellowship. He has received fees for consultancy work from Novartis, Bayer, AstraZeneca, Menarini, Nycomed, Gilead, Boehringer Ingelheim, Teva, Rowex and

Mundipharma. He has received speaker's fees from Pfizer, Menarini, GSK, Bayer, MSD and Novartis. He has travelled to international symposia as a guest of Boehringer Ingelheim and Novartis.

Abbreviations

ANOVA	Analysis of Variance
BMI	Body Mass Index
CF	Cystic Fibrosis
CFQ-R	Cystic Fibrosis Questionnaire Revised
CFTR	Cystic Fibrosis Transmembrane conductance Regulator
CT	Computed Tomography
ELISA	Enzyme linked immunosorbent assay
FEV1	Forced Expiratory Volume in one second
IL	Interleukin
IV	Intravenous
PWCF	Patients with cystic fibrosis

Abstract

Background: Ivacaftor produces significant clinical benefit in patients with cystic fibrosis (CF) with the G551D mutation. Prevalence of this mutation at Cork CF Centre is 23%. This study assessed the impact of CFTR modulation on multiple modalities of patient assessment.

Methods: Thirty three patients with the G551D mutation were assessed at baseline and prospectively three monthly for one year post initiation of ivacaftor. Change in ultra-low dose chest CT, blood inflammatory mediators, and sputum microbiome were assessed.

Results: Significant improvements in FEV₁, BMI and sweat chloride were observed post-ivacaftor. Improvement in ultra-low dose CT scores were observed after treatment with significant mean reductions in total Bhalla score ($p < 0.01$), peri-bronchial thickening ($p = 0.035$) and extent of mucus plugging ($p < 0.001$). Reductions in circulating inflammatory markers, including IL-1 β , IL-6, and IL-8 were demonstrated. There was a 30% reduction in the relative abundance of *Pseudomonas* spp. and an increase in the relative abundance of bacteria associated with more stable community structures. Post-treatment community richness increased significantly ($p = 0.03$).

Conclusions: Early and sustained improvements on ultra-low-dose CT scores suggest it may be a useful method of evaluating treatment response. It was paralleled improvement in symptoms, circulating inflammatory markers, and changes in the lung microbiota.

Introduction

Ivacaftor is the first treatment which treats the underlying cause of cystic Fibrosis (CF) by enhancing cystic fibrosis conductance transmembrane regulatory (CFTR) function in the setting of class III and IV mutations (1-3). In class III mutations, the CFTR channel is located at the correct site at the cell surface but fails to open and close normally. The G551D mutation is the most common class III mutation with a worldwide prevalence of 4-5% (4). There is significant regional variation (5). Prevalence of the G551D mutation in Cork CF Centre is 23%, making it uniquely placed to offer a single centre insight on treatment response. Ivacaftor treatment results in significant improvement in lung function (FEV_1), increase in body mass index (BMI), improved respiratory symptoms, reduction in sweat chloride concentration, and reduction in pulmonary exacerbations in patients with CF with the G551D mutation (1, 2).

Chest CT changes including mild bronchiectasis can be demonstrated in people with CF (PWCF) who have a normal FEV_1 . CT evidence of disease progression has been observed in individuals whose FEV_1 has remained stable over time. A small study using standard CT protocols before and after one year of ivacaftor demonstrated improvement (6). Low dose CT scanning has not been used prospectively to evaluate treatment effect. We assessed the effect of ivacaftor on low dose chest CT.

Microbiology studies have suggested subtle changes in the lung microbiome after commencement of ivacaftor (7), thus we assessed the lung microbiota after treatment. Recent data have demonstrated no significant change in sputum cytokines after commencement of ivacaftor. We assessed change in circulating inflammatory markers after treatment. We hypothesise that CFTR modulatory therapy may result in improvement in low dose chest CT, circulating inflammatory mediators and changes in the lung microbiota.

Methods

All patients with CF aged six years or older with at least one copy of the G551D mutation attending Cork CF centre were started on Ivacaftor post March 2013 and followed prospectively, for a mean period of follow-up of 12 months. Prevalence of the G551D mutation at Cork CF centre is 23%, with 51 of 220 patients carrying at least one copy of the G551D mutation. Thirty three patients with the G551D mutation consented to participate. Eight children were too young to receive ivacaftor, 6 patients had already commenced ivacaftor either as part of a clinical trial or on a named patient (compassionate use) basis, two patients were post lung transplantation and three were undecided as to whether they wished to start treatment. According to the UK CF trust annual report 2015, there are 32 patients with the G551D in Northern Ireland, representing 8% of the CF population. According to the CF Registry of Ireland annual report there are 93 patients with the G551D mutation in the Republic of Ireland, representing 11.3% of the CF population. Thus this patient group represents approximately one quarter of patients with the G551D mutation on the island of Ireland. Ethical approval was obtained for the CORK (Clinical Outcome in Real-world Kalydeco) study, from the Clinical Research Ethics Committee of the Cork Teaching Hospitals. Ivacaftor-naïve patients with CF attended for assessment when clinically stable. Spirometry was performed according to ERS/ATS guidelines using CareFusion MicroLab™ spirometer which is calibrated on a regular basis (8). Sweat-testing was performed using a Macroduct™ system in accordance with manufacturer's guidelines. Modified shuttle walk test was performed at visits. Patients aged 14 and older completed Cystic Fibrosis Questionnaire Revised (CFQ-R) and for patients aged 6 -14 parents completed care-giver CFQ-R (9). Participants were assessed on a three monthly basis after ivacaftor. The numbers

of courses of intravenous antibiotic (IV) for pulmonary exacerbations were recorded prospectively for 12 months after ivacaftor and compared with the number of courses of IV antibiotics 12 months before commencing ivacaftor.

Radiology

Adapted ultra-low dose chest CT were performed (mean effective radiation dose 0.08 mSv), using a previously validated protocol (10), at baseline and after 3, 6 and 12 months of treatment on participants aged 16 and older. Chest CT scans were scored by consensus of two experienced consultant radiologists using a Bhalla scoring system (11).

Sputum

Adult patients produced a sputum sample at baseline when clinically stable, before commencing ivacaftor and at three monthly clinic review post ivacaftor when able to expectorate.

Blood samples

Blood samples were collected on all patients in bottles containing sodium citrate with the plasma layer separated and stored at -80 °C. Circulating inflammatory markers - including *IL-1 β* , *IL-6*, *IL-8*, *IL-10*, *TNF- α* and *CRP*- were measured using a multiplex enzyme linked immunosorbent assay (ELISA) (MesoScale Discovery (MSD) platform) according to the manufacturer's guidelines (12, 13).

Molecular detection - Illumina MiSeq sequencing

Processing of sputum samples and sequence library preparation is described in detail within the Online Supplement. 16S rRNA marker gene sequencing was performed on the Illumina MiSeq platform (Illumina, CA, USA) targeting the V4 the hyper-variable region of the 16S rRNA gene as previously described (14). Intra-sample similarities/differences were assessed through relative abundance changes in microbial taxa between visit time-points, sample richness (number of counted taxa) and diversity (Shannon Wiener Index).

Statistical Analysis

Data was analysed using SPSS version 22.0. A mean post follow up value was calculated for each parameter for each patient (mean of available 3, 6, 9 and 12 month values) and this post value was compared to the value before commencing ivacaftor. Blood inflammatory marker data was \log_{10} transformed before analysis. Paired sample t test was used to evaluate mean change from baseline for normally distributed variables. Paired Wilcoxon signed rank test was used to evaluate the change in non-normally distributed data. Repeated measures ANOVA with a Bonferroni correction for multiple comparisons were used to compare changes in chest CT score. Pearson's and Spearman's Rank correlation coefficients, as appropriate to the distribution, were used to evaluate correlation between clinical parameters, blood biomarkers and chest CT scores.

Results

Clinical

Twenty adults and 13 paediatric patients participated. Table 1 summarises baseline characteristics. The mean age of the cohort was 21.6 years and 70% of participants were male. The mean baseline FEV₁ % predicted was 75.21% (*SD* 20.7). Mean baseline sweat chloride was 101 mmol/l (*SD* 14.7). The majority (85%) of patients had the F508del mutation as their second mutation. One patient was homozygous for the G551D mutation. All other patients had a class I or II mutation as their second mutation.

After commencement of therapy a 10.3% mean increase in FEV₁ % predicted was observed ($p < 0.001$) and a 58 mmol/l mean reduction in sweat chloride were observed after treatment ($p < 0.001$) (Figure 1). After 1 year of treatment 83 % of patients had a sweat chloride below the level considered diagnostic for CF (60 mmol/l) (supplemental data e-figure 2). No significant relationship was observed between the magnitude of change in FEV₁ and the magnitude of change in sweat chloride after 3, 6, 9 or 12 months of treatment (e-figure 3). A 76 % reduction in pulmonary exacerbations requiring intravenous antibiotics was observed in the first year of therapy compared to the year before treatment; with a reduction in the mean number of exacerbations per patients from 0.88 to 0.21 ($p = 0.006$). A significant 109 metre mean increase in modified shuttle walk test ($p = 0.001$) and a 1.2 kg/m² significant mean increase in BMI ($p < 0.001$) were observed after ivacaftor (Figure 2). These results are in keeping with those observed in previous studies (1, 7).

A 17.5 point mean increase in adult ($p < 0.001$) and an 8.8 point mean increase in caregiver completed CFQ-R Respiratory Domain ($p = 0.08$) were observed (e-Figure 4). Changes in other domains of the CFQ-R can be found in the online supplement (e-Table 1).

Radiology

Eighteen adults had a low dose chest CT performed before ivacaftor and after 3, 6 and 12 months of treatment, with CT findings summarised in Table 2. In this group a 12% mean increase in FEV₁ % predicted ($p < 0.01$), 58 mmol/l mean reduction in sweat chloride ($p < 0.01$) and 1.6 Kg/m² mean increase in BMI were observed. Repeat measures ANOVA demonstrated significant mean reductions in total Bhalla score ($p < 0.01$), peri-bronchial thickening ($p = 0.035$), and extent of mucus plugging ($p < 0.01$) with treatment. There was no statistically significant change in the severity and extent of bronchiectasis, number of bullae, emphysema, presence of sacculation or abscesses and the generations of bronchial divisions involved in bronchiectasis and plugging (Table 2). Post hoc testing using a Bonferroni correction for multiple comparisons demonstrated significant improvement from baseline in total Bhalla score ($p < 0.01$) and mucus plugging ($p < 0.01$) after 3, 6 and 12 months. E-Images 1 and 2 illustrate representative chest CT's before and after treatment.

Culture independent analysis

Analysis of airway microbial community composition was performed for a subset of patients (n=14) who provided a sputum for pre- and at least one post-treatment sputum sample. For patients with more than one post-treatment sample, we analysed the last sample collected representing the change from baseline (pre-treatment sample). Five main taxa, which accounted for >1% of total sequence reads in each of the corresponding samples, dominated the overall community in both pre- and post-treatment sample groups (Figure 3a). Following treatment, there was a 30% (68% to 53%) reduction in the relative proportion of *Pseudomonas* spp. within the community. In contrast, there was an overall increase in the

relative proportion of *Streptococcus* spp., *Rothia* spp., *Haemophilus* spp. and *Prevotella* spp., ranging from 19% to 80% post-treatment (Figure 3a).

Taxonomic richness (i.e. the number of taxa present in a sample at a particular taxonomic level) increased significantly following treatment ($p = 0.031$; paired Student's t-test) (Figure 3b). We observed an increase in community diversity post-treatment but this did not reach statistical significance ($p = 0.069$; Mann-Whitney test) (Figure 3c).

Circulating inflammatory markers

Significant reductions in circulating \log_{10} IL-6 ($p < 0.01$), \log_{10} IL-8 ($p < 0.01$), \log_{10} IL-10 (< 0.01), \log_{10} IL-1 β ($p < 0.01$) and \log_{10} CRP ($p = 0.015$) were observed after treatment (e-figure 6). A non-significant reduction in \log_{10} TNF- α was observed after commencement of treatment ($p = 0.06$).

Discussion

This is the first study to utilise ultra-low dose chest CT (mean dose 0.08 mSv per scan) to serially examine the ivacaftor response over a one year period, allowing an assessment of the key mechanisms underlying clinical response and assessing its utility in a clinical setting to monitor CFTR modulatory therapy response. Significant improvements in ultra-low dose chest CT were observed early, after three months of treatment, with further improvements noted after 1 year of therapy. The greatest improvements on chest CT were in the extent of mucus plugging. This is consistent with *in vitro* studies where ivacaftor enhanced airway surface liquid and ciliary beat frequency (15, 16). The limitation of using FEV₁ to assess treatment response in particular in patients with relatively preserved lung function is well

recognised (17). Thus we suggest ultra-low dose chest CT may represent a biomarker of early and sustained treatment response post CFTR modulation. It may be a useful potential new outcome measure in clinical care with broad application across CF sites. The growing awareness that patients with CF are at increased risk of certain neoplasms supports using low dose CT to reduce this risk (18, 19).

There was no statistically significant change in bronchiectasis on chest CT after ivacaftor therapy in contrast to a previous smaller study which included adults and children (6). Our study supports that in established lung damage bronchiectasis is not reversible with CFTR modulatory therapy. It remains to be established if treatment with ivacaftor will delay or prevent the development of bronchiectasis in those who start treatment early.

We observed significant improvements in lung function, weight, walk test, and CFQ-R after commencement of ivacaftor. The improvement in lung function was in keeping with that observed in the clinical trials and larger than that observed in other observational studies in people on treatment outside of clinical trials (7). This may be due to the fact that our cohort had a lower baseline FEV₁ than those in other observational studies. The improvement in respiratory domain of the CFQ-R was larger than that observed in the clinical trials (1, 2). In keeping with previous work (n=24) no correlation was observed between the change in FEV₁ % predicted and change in sweat chloride at any of the time points suggesting it is a poor marker of treatment response (20).

We have demonstrated that following ivacaftor treatment, significant changes occur in the microbial community composition. The reduction in the relative abundance for members of *Pseudomonas* spp. is in keeping with previous data (7). The increase in *Streptococcus* spp., as

well as in the obligate anaerobic taxa *Prevotella* spp. and *Veillonella* spp., demonstrates a potentially important clinical trend. The increase taxonomic richness and movement towards increased community diversity post-treatment is important given previous work demonstrating a relationship between greater lung microbial diversity and better lung function (21). Significant changes in the community composition of the airway microbiota in patients with CF have been shown to occur during the progression of the disease (22). These changes include the narrowing in the spectrum of bacterial taxa, associated with a reduction in taxonomic richness and community diversity. The reason behind such a change in the community composition has been hard to elucidate and multifactorial, though increased patient age and antimicrobial treatment burden in chronically colonized patients (23) has been shown to play a significant part (21, 23). The subtle reversal towards a more "stable" microbiota similar to a "healthier" CF lung microbiome is important and may reflect disease reversal. That said a significant 76% reduction in intravenous antibiotic requirements was observed in the year after ivacaftor which also would contributed to this finding. Changes within the lung environment may alter the lung environment sufficiently to driving such change (24).

We observed significant reduction in a number of circulating inflammatory markers. This 'real-world' finding is consistent with the results from a group of patients in the clinical trials which demonstrated a significant reduction in circulating neutrophil count, IL-8, CRP and IgG after 24 weeks of treatment (25). That said another real-world cohort failed to demonstrate a significant change in sputum cytokines in patients with CF treated with ivacaftor (7). Inflammation in the CF lung is characterised by an excess influx of polymorph nuclear neutrophils (PMNs) (26-29). Exaggerated inflammation develops early in the course of CF, with elevated levels of inflammatory markers being demonstrated in the lung of

infants with CF in the absence of overt infection (26, 27, 30-33). Previous studies have demonstrated elevated levels of circulating inflammatory markers, including IL-2, IL 6, IL-8 and TNF- α in patients with CF compared to control cohorts (34-39) . Similarly some studies have demonstrated reduction in circulating inflammatory markers after antibiotic therapy for pulmonary exacerbations (40). (Whether the reduction seen in our cohort is due solely to a decrease in pulmonary exacerbations observed in our cohort or augmented by potential changes in immune function post restoration of CFTR function remains to be evaluated given that studies have demonstrated improved neutrophil function after ivacaftor therapy (41, 42).

Given the sustained improvements in chest CT observed from 3 months after commencement of ivacaftor - in particular improved mucus plugging and peri-bronchial thickening we suggest that enhanced mucus clearance is a key mechanism underlying the increase in lung function and reduction in pulmonary exacerbations observed in patients treated with ivacaftor. This is consistent with in vitro studies where ivacaftor resulted in improved airway surface liquid and ciliary beat frequency (15, 16).

The subsequent improvement in symptoms, reduction in circulating inflammatory markers, and subtle changes in the lung microbiome are likely secondary factors contributing to this improvement.

Limitations

A limitation of this study is that it is observational in nature without a control group who did not receive ivacaftor treatment. However, the benefits of ivacaftor relative to placebo have been well demonstrated in existing trials, the observed improvements are similar to those reported in the above trials and would be disproportionate to changes expected in untreated cohort. We avoided recruitment sample related variability given that we included the entire

cohort of patients attending our designated referral centre for the region. All eligible patients received the drug as it was funded by the state and not dependant on health insurance status.

Conclusion

This study demonstrates sustained improvement after ivacaftor across multiple modalities of assessment including multiple clinical parameters, ultra-low dose chest CT, blood inflammatory markers and lung microbiome. It suggests the potential utility of ultra-low dose chest CT as an approach for assessing treatment response.

References

1. Ramsey BW, Davies J, McElvaney NG, Tullis E, Bell SC, Dřevínek P, et al. A CFTR potentiator in patients with cystic fibrosis and the G551D mutation. *New England Journal of Medicine*. 2011;365(18):1663-72.
2. Davies JC, Wainwright CE, Canny GJ, Chilvers MA, Howenstine MS, Munck A, et al. Efficacy and safety of ivacaftor in patients aged 6 to 11 years with cystic fibrosis with a G551D mutation. *American Journal of Respiratory and Critical Care Medicine*. 2013;187(11):1219-25.
3. De Boeck K, Munck A, Walker S, Faro A, Hiatt P, Gilmartin G, et al. Efficacy and safety of ivacaftor in patients with cystic fibrosis and a non-G551D gating mutation. *Journal of Cystic Fibrosis*. 2014.
4. Bobadilla JL, Macek M, Jr., Fine JP, Farrell PM. Cystic fibrosis: a worldwide analysis of CFTR mutations--correlation with incidence data and application to screening. *Hum Mutat*. 2002;19(6):575-606.
5. De Boeck K, Zolin A, Cuppens H, Olesen H, Viviani L. The relative frequency of CFTR mutation classes in European patients with cystic fibrosis. *Journal of Cystic Fibrosis*. 2014.
6. Sheikh SI, Long FR, McCoy KS, Johnson T, Ryan-Wenger NA, Hayes Jr D. Computed tomography correlates with improvement with ivacaftor in cystic fibrosis patients with G551D mutation. *Journal of Cystic Fibrosis*. 2014.
7. Rowe SM, Heltshe SL, Gonska T, Donaldson SH, Borowitz D, Gelfond D, et al. Clinical Mechanism of the Cystic Fibrosis Transmembrane Conductance Regulator Potentiator Ivacaftor in G551D-mediated Cystic Fibrosis. *American Journal of Respiratory and Critical Care Medicine*. 2014;190(2):175-84.

8. Miller MR, Hankinson J, Brusasco V, Burgos F, Casaburi R, Coates A, et al. Standardisation of spirometry. *Eur Respir J*. 2005;26(2):319-38.
9. Quittner AL, Buu A, Messer MA, Modi AC, Watrous M. Development and validation of The Cystic Fibrosis Questionnaire in the United States: a health-related quality-of-life measure for cystic fibrosis. *CHEST Journal*. 2005;128(4):2347-54.
10. O'Connor OJ, Vandeleur M, McGarrigle AM, Moore N, McWilliams SR, McSweeney SE, et al. Development of Low-Dose Protocols for Thin-Section CT Assessment of Cystic Fibrosis in Pediatric Patients 1. *Radiology*. 2010;257(3):820-9.
11. Bhalla M, Turcios N, Aponte V, Jenkins M, Leitman B, McCauley D, et al. Cystic fibrosis: scoring system with thin-section CT. *Radiology*. 1991;179(3):783-8.
12. Breen EC, Reynolds SM, Cox C, Jacobson LP, Magpantay L, Mulder CB, et al. Multisite comparison of high-sensitivity multiplex cytokine assays. *Clinical and Vaccine Immunology*. 2011;18(8):1229-42.
13. Chowdhury F, Williams A, Johnson P. Validation and comparison of two multiplex technologies, Luminex[®] and Mesoscale Discovery, for human cytokine profiling. *Journal of immunological methods*. 2009;340(1):55-64.
14. Lundberg DS, Yourstone S, Mieczkowski P, Jones CD, Dangl JL. Practical innovations for high-throughput amplicon sequencing. *Nat Methods*. 2013;10(10):999-1002.
15. Yu H, Burton B, Huang C-J, Worley J, Cao D, Johnson JP, et al. Ivacaftor potentiation of multiple CFTR channels with gating mutations. *Journal of Cystic Fibrosis*. 2012;11(3):237-45.
16. Van Goor F, Hadida S, Grootenhuis PD, Burton B, Cao D, Neuberger T, et al. Rescue of CF airway epithelial cell function in vitro by a CFTR potentiator, VX-770. *Proceedings of the National Academy of Sciences*. 2009;106(44):18825-30.
17. EMA. http://www.ema.europa.eu/docs/en_GB/document_library/Scientific_guideline/2009/12/WC500017055.pdf.
18. Murphy KP, O'Connell OJ, O'Connor OJ, Plant BJ, Maher MM. Cumulative radiation exposure to abdominal organs in patients with cystic fibrosis should not be forgotten. *Am J Respir Crit Care Med*. 2014;190(8):961-2.
19. O'Connell OJ, McWilliams S, McGarrigle A, O'Connor OJ, Shanahan F, Mullane D, et al. Radiologic imaging in cystic fibrosis: cumulative effective dose and changing trends over 2 decades. *Chest*. 2012;141(6):1575-83.
20. Barry PJ, Jones AM, Webb AK, Horsley AR. Sweat chloride is not a useful marker of clinical response to Ivacaftor. *Thorax*. 2014;69(6):586-7.
21. Cox MJ, Allgaier M, Taylor B, Baek MS, Huang YJ, Daly RA, et al. Airway microbiota and pathogen abundance in age-stratified cystic fibrosis patients. *PLoS One*. 2010;5(6):e11044.
22. Paganin P, Fiscarelli EV, Tuccio V, Chiancianesi M, Bacci G, Morelli P, et al. Changes in Cystic Fibrosis Airway Microbial Community Associated with a Severe Decline in Lung Function. *PLoS ONE*. 2015;10(4):e0124348.
23. Zhao J, Schloss PD, Kalikin LM, Carmody LA, Foster BK, Petrosino JF, et al. Decade-long bacterial community dynamics in cystic fibrosis airways. *Proc Natl Acad Sci U S A*. 2012;109(15):5809-14.

24. Shah VS, Ernst S, Tang XX, Karp PH, Parker CP, Ostedgaard LS, et al. Relationships among CFTR expression, HCO₃⁻ secretion, and host defense may inform gene- and cell-based cystic fibrosis therapies. *Proc Natl Acad Sci U S A*. 2016;113(19):5382-7.
25. Seliger V, Accurso F, Konstan M, Dong Q, Lubarsky B, Mueller P. Effect of ivacaftor on circulating inflammatory indices in CF patients with the G551D-CFTR mutation. *Pediatric pulmonology*. 2013;48(s36):298-9.
26. Cantin A. Cystic fibrosis lung inflammation: early, sustained, and severe. *American Journal of Respiratory and Critical Care Medicine*. 1995;151(4):939-41.
27. Khan TZ, Wagener JS, Bost T, Martinez J, Accurso FJ, Riches D. Early pulmonary inflammation in infants with cystic fibrosis. *American Journal of Respiratory and Critical Care Medicine*. 2011;151(4).
28. Regelman WE, Siefferman CM, Herron JM, Elliott GR, Clawson CC, Gray BH. Sputum peroxidase activity correlates with the severity of lung disease in cystic fibrosis. *Pediatric pulmonology*. 1995;19(1):1-9.
29. Birrer P, McElvaney N, Rudeberg A, Sommer CW, Liechti-Gallati S, Kraemer R, et al. Protease-antiprotease imbalance in the lungs of children with cystic fibrosis. *American Journal of Respiratory and Critical Care Medicine*. 1994;150(1):207-13.
30. Balough K, McCubbin M, Weinberger M, Smits W, Ahrens R, Fick R. The relationship between infection and inflammation in the early stages of lung disease from cystic fibrosis. *Pediatric pulmonology*. 1995;20(2):63-70.
31. Konstan MW, Hilliard KA, Norvell TM, Berger M. Bronchoalveolar lavage findings in cystic fibrosis patients with stable, clinically mild lung disease suggest ongoing infection and inflammation. *American Journal of Respiratory and Critical Care Medicine*. 1994;150(2):448-54.
32. Muhlebach MS, Noah TL. Endotoxin activity and inflammatory markers in the airways of young patients with cystic fibrosis. *American Journal of Respiratory and Critical Care Medicine*. 2002;165(7):911-5.
33. Dakin CJ, Numa AH, Wang H, Morton JR, Vertzyas CC, Henry RL. Inflammation, infection, and pulmonary function in infants and young children with cystic fibrosis. *American Journal of Respiratory and Critical Care Medicine*. 2002;165(7):904-10.
34. Tirelli AS, Colombo C, Torresani E, Fortunato F, Biffi A, Cariani L, et al. Effects of treatment in the levels of circulating cytokines and growth factors in cystic fibrosis and dialyzed patients by multi-analytical determination with a biochip array platform. *Cytokine*. 2013;62(3):413-20.
35. Dean TP, Dai Y, Shute JK, Church MK, Warner JO. Interleukin-8 concentrations are elevated in bronchoalveolar lavage, sputum, and sera of children with cystic fibrosis. *Pediatric research*. 1993;34(2):159-61.
36. Nixon LS, Yung B, Bell SC, Stuart Elborn J, Shale DJ. Circulating immunoreactive interleukin-6 in cystic fibrosis. *American Journal of Respiratory and Critical Care Medicine*. 1998;157(6):1764-9.
37. Norman D, Elborn J, Cordon S, Rayner R, Wiseman M, Hiller E, et al. Plasma tumour necrosis factor alpha in cystic fibrosis. *Thorax*. 1991;46(2):91-5.
38. Schmitt-Grohé S, Naujoks C, Bargon J, Wagner TO, Schubert R, Hippe V, et al. Interleukin-8 in whole blood and clinical status in cystic fibrosis. *Cytokine*. 2005;29(1):18-23.
39. Corvol H, Fitting C, Chadelat K, Jacquot J, Tabary O, Boule M, et al. Distinct cytokine production by lung and blood neutrophils from children with cystic fibrosis. *American Journal of Physiology-Lung Cellular and Molecular Physiology*. 2003;284(6):L997-L1003.
40. Tirelli AS, Colombo C, Torresani E, Fortunato F, Biffi A, Cariani L, et al. Effects of treatment in the levels of circulating cytokines and growth factors in cystic fibrosis and dialyzed patients by multi-analytical determination with a biochip array platform. *Cytokine*. 2013;62(3):413-20.
41. Pohl K, Hayes E, Keenan J, Henry M, Meleady P, Molloy K, et al. A neutrophil intrinsic impairment affecting Rab27a and degranulation in cystic fibrosis is corrected by CFTR potentiator therapy. *Blood*. 2014.

42. Bratcher PE, Rowe SM, Reeves G, Roberts T, Szul T, Harris WT, et al. Alterations in blood leukocytes of G551D-bearing cystic fibrosis patients undergoing treatment with ivacaftor. *Journal of Cystic Fibrosis*. 2015.

ACCEPTED MANUSCRIPT

Table 1. Baseline Characteristics

	Mean (SD)
	N = 33
Gender (% male)	70
Age (years)	21.6
FEV1 (% predicted)	75.21 (20.7)
Weight (Kg)	51.26 (19.7)
Walk test (metres)	1002 (320)
Sweat test (mmol/l)	101 (14.7)
Mutation (%)	
G551D/F508del	85%
G551D/G551D	3%
G551D/3028delA	3%
G551d/1717-1G →A	3%
G551D/E56K	3%
G551D/R553x	3%

ACCEPTED MANUSCRIPT

Table 2. Chest CT Bhalla Score

Bhalla score (range)	Baseline	3 months	6 months	12 months	<i>P value</i>
	Mean score (SD) N = 18	Mean score (SD) N = 18	Mean score (SD) N = 18	Mean score (SD) N = 18	
Total Bhalla score (0-25)	12.56 (4.2)	10.94 (3.6)	10.22 (3.4)	10.33 (3.4)	<0.01
Peri-bronchial thickening (0-3)	1.11 (0.8)	0.89 (0.7)	0.83 (0.7)	0.72 (0.6)	0.035
Severity of bronchiectasis (0-3)	2.06 (0.9)	2.11 (0.9)	2.06 (0.9)	2.06 (0.9)	0.33
Extent of bronchiectasis	2.83 (0.4)	2.83 (0.4)	2.78 (0.4)	2.83 (0.4)	<0.01
Sacculation or abscesses (0-3)	0 (0)	0 (0)	0 (0)	0 (0)	1
Generations of bronchial divisions involved (0-3)	2.44 (0.7)	2.4 (0.8)	2.44 (0.7)	2.4 (0.8)	0.7
Number of bullae (0-3)	0.67 (1.1)	0.5 (0.9)	0.5 (0.9)	0.44 (0.9)	0.3
Emphysema (0-2)	1.17 (0.7)	0.94 (0.7)	0.7 (0.6)	1.0 (0.6)	0.15

Collapse/consolidation (0-2)	0.44 (0.6)	0.28 (0.6)	0.22 (0.4)	0.22 (0.4)	0.1
---------------------------------	------------	------------	------------	------------	-----

ACCEPTED MANUSCRIPT

Figure 1 Change in FEV1 % predicted and sweat chloride concentration at baseline and after 1 year of ivacaftor therapy

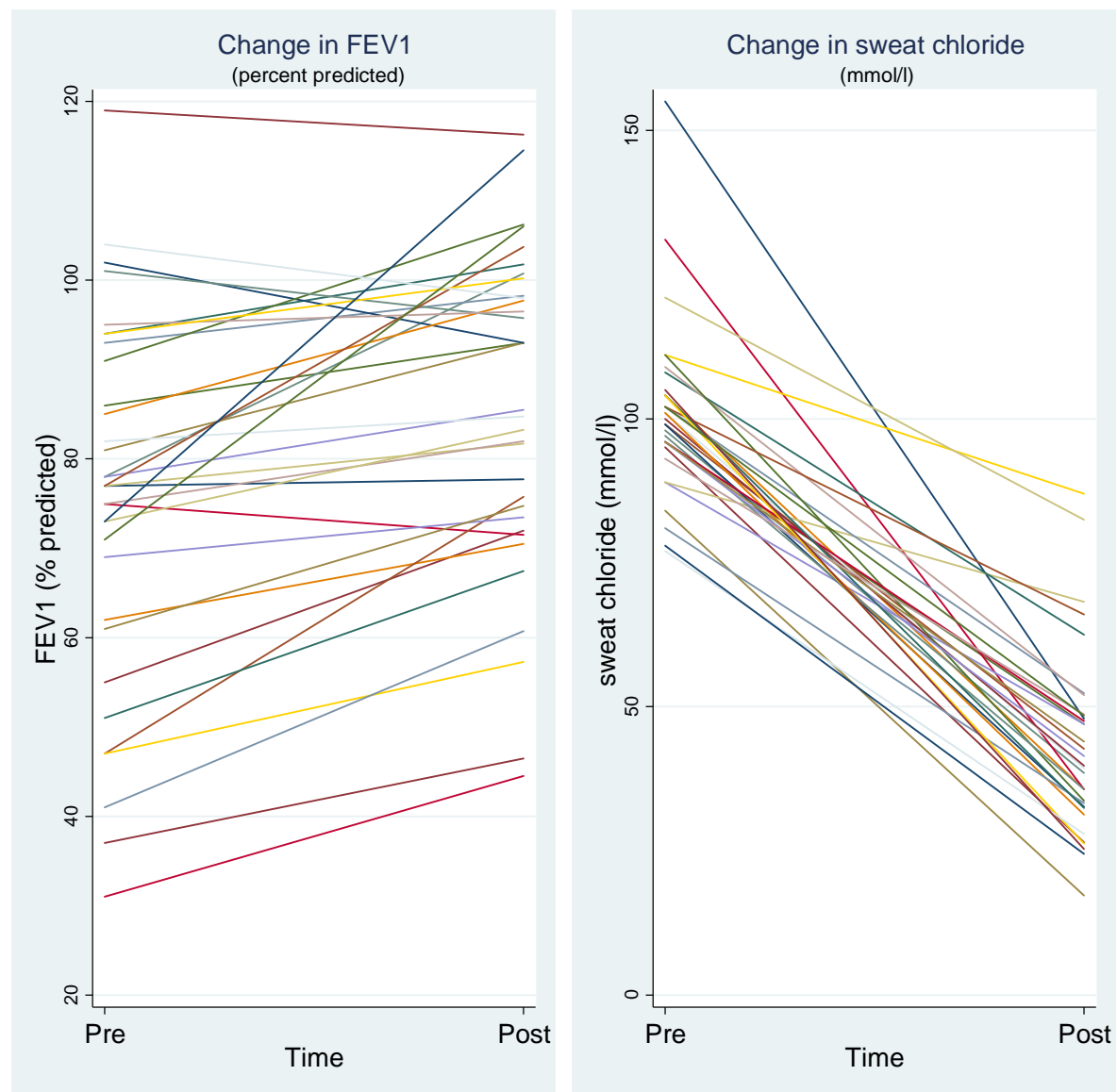


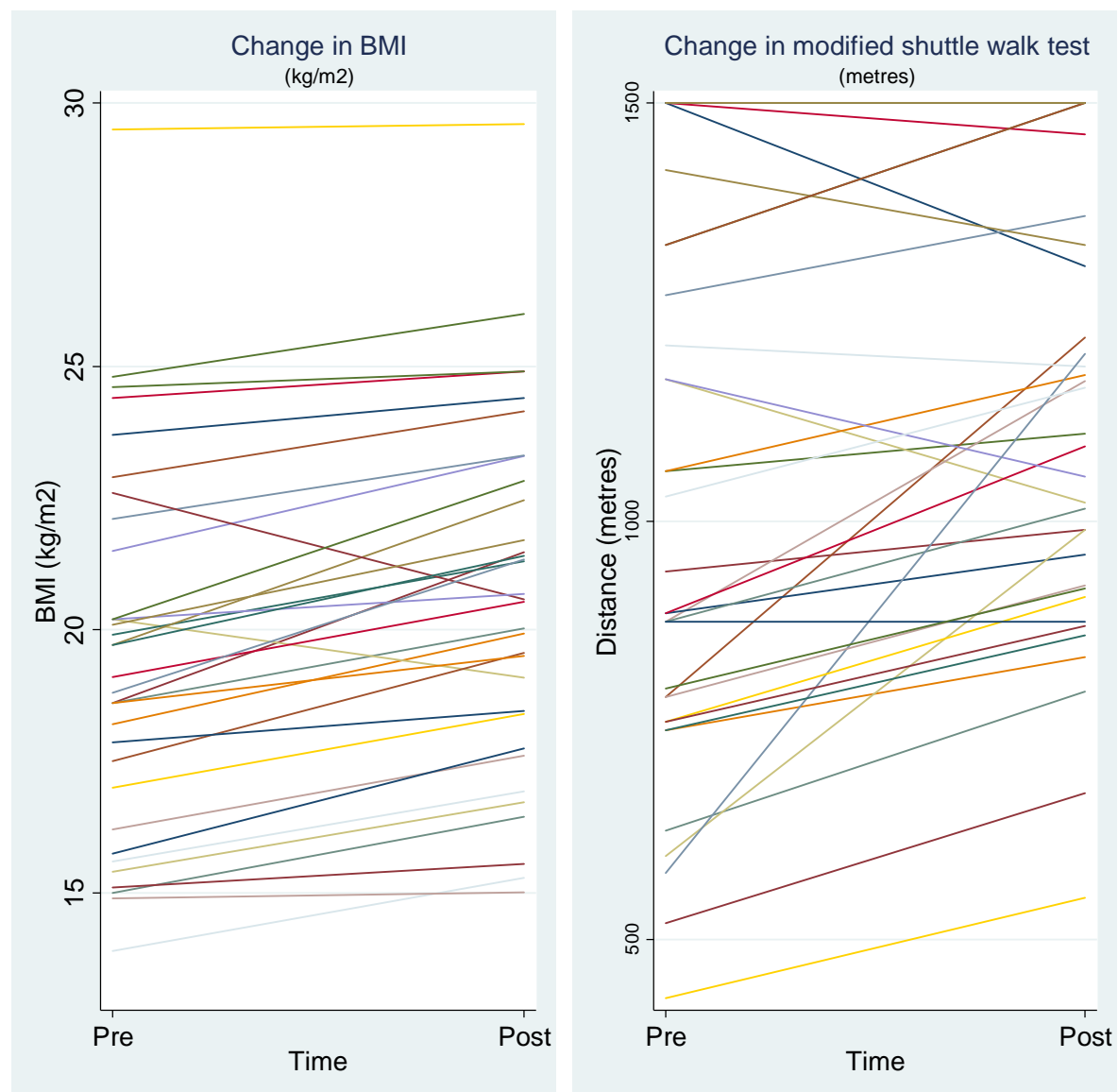
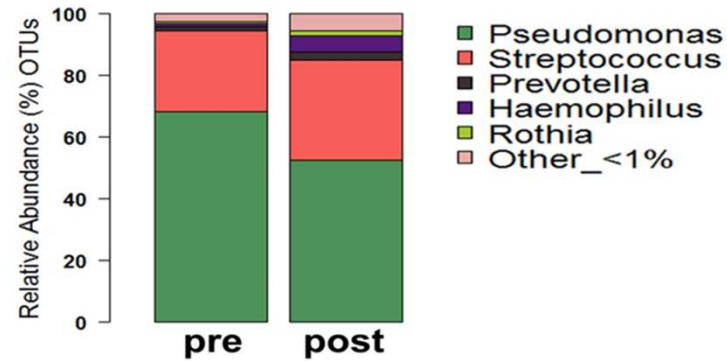
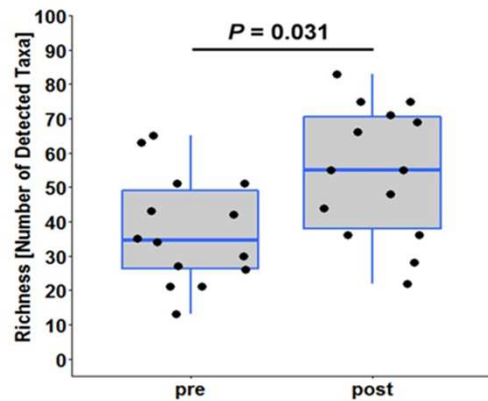
Figure 2 Change in BMI and modified shuttle walk test after ivacaftor

Figure 3 (a) Stacked bar representing the relative abundance of genera accounting for the total sequence count in each group, (b) taxonomic richness and (c) Shannon Wiener Index of diversity. The top and bottom boundaries of each box indicate 75th and 25th quartile values, respectively, with the blue line inside each box representing the median (50th quartile). The ends of the whiskers indicate the 95% CI around the median. Difference between normally distributed variables (richness) was evaluated using a paired t-test. Difference between non-normally distributed variables (Shannon Wiener diversity) was assessed using Mann-Whitney test. $P < 0.05$ denotes statistical significance.

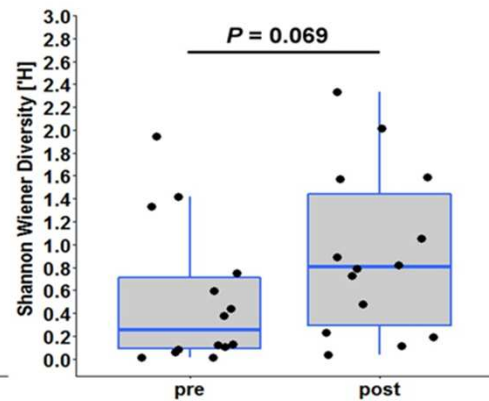
a.



b.



c.



e-Appendix 1.**Radiology**

CT technique and image reconstruction

All studies were acquired using a 64-slice multidetector CT scanner (General Electric Discovery CT 750 HD; GE Healthcare, GE Medical Systems, Milwaukee, WI, USA) without intravenous contrast material.

7-section low-dose protocol

A modified 7-section, low-dose axial CT protocol previously validated at our institution was used for the pre-treatment and first 12-month quarterly studies.¹⁷

Single anteroposterior and mediolateral localizer radiographs were used to identify 5 levels, evenly spaced, at which images were acquired. Images were obtained with the patient at end-inspiration through the lung apices, aortopulmonary window, carina, and at the widest cardiac and thoracic diameters. 2 further images were obtained with the patient in full expiration at the aortopulmonary window and at the widest cardiac diameter. The following parameters were used: tube voltage of 120 kV; gantry rotation time of 0.4 seconds; field of view (FOV) of 32cm; and z-axis automatic tube current modulation with minimum and maximum tube current thresholds set at 10 and 100 mA with a tolerated noise index of 29HU. Images were acquired at each of the 7 levels at a slice thickness of 0.625mm and reconstructed to a slice thickness of 1.25 mm with the standard departmental protocol employing hybrid IR: 70% filtered back projection and 30% adaptive statistical iterative reconstruction (ASIR)(GE Healthcare, GE Medical Systems, Milwaukee, USA).

Full-volume low-dose protocol

A low-dose volumetric protocol was used to acquire the 24-month surveillance CT. the following technical parameters in combination with model-based iterative reconstruction (MBIR); Veo (GE Healthcare, GE Medical Systems, Milwaukee, USA) were used: tube voltage of 80 kV; tube current of 20mA; gantry rotation time of 0.4 seconds; pitch factor of 1.375; and FOV of 32cm.

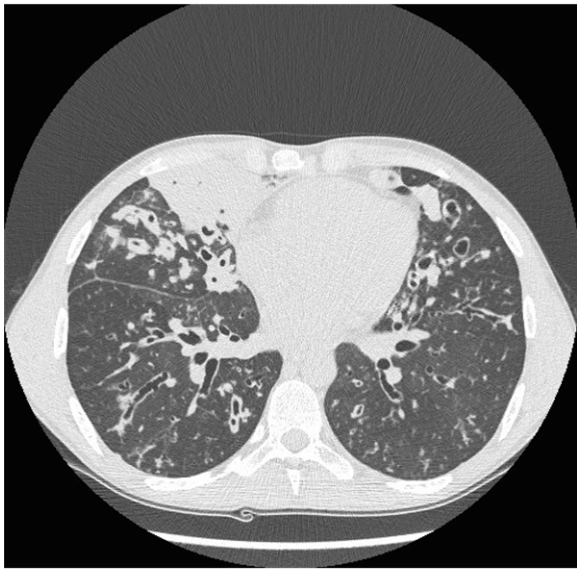
Scanning was performed at end-inspiration from the lung apices to the bases, including the costophrenic recesses. No additional expiratory phase imaging was performed. Images were acquired at a slice thickness of 0.625mm and reconstructed at a final slice thickness of 1.25 mm.

Quantification of lung disease

Disease severity was scored independently by two readers (MMM and OJOC) using a validated scoring system (Bhalla score). Both readers had significant prior experience of MBIR-reconstructed images. To minimize the effects of recall bias, all datasets were anonymized and reviewed in a random order. In addition, a 6-week delay was instituted between the review of the baseline and 1-year LD-ASIR studies and the 2-year LD-MBIR studies. Images were reviewed on lung window settings (window width, 1500HU; window level: -500HU) on the picture archiving and communication system using axial reformations (Impax 6.5.3; Agfa healthcare, Morstel, Belgium).

The presence and severity of 9 morphological changes were evaluated including: severity of bronchiectasis; peribronchial thickening; extent of bronchiectasis (number of bronchopulmonary segments); extent of mucus plugging (number of lung segments); abscesses or sacculations (number of lung segments); generations of the bronchial divisions involved; number of bullae; air trapping (number of lung segments); and collapse/consolidation. A score of 0 to 3 (0: absent; 1: mild; 2: moderate; 3: severe) was assigned to each category to give a total score ranging from 0 to 25. A score of 0 indicated that no abnormality was detected.

e-Figure 1. Interval resolution of right middle lobe medial segmental consolidation and collapse and reduction in the degree of peribronchial wall thickening and foci of mucous plugging in the left and right lower lobes. Persistent residual mucous plugging in the lingula anteriorly.



e-Figure 2. Interval reduction in degree of peribronchial wall thickening, mucous plugging and tree in bud opacification, with the degree of bronchiectasis remaining unchanged.



Blood inflammatory mediators

Blood samples were diluted 1:1 with PBS and separated using a ficoll banding. The plasma was frozen immediately at -80°C. Plasma samples were subsequently thawed on ice. Circulating inflammatory mediators were measured using a mesoscale discovery (MSD) platform in keeping with manufacturer's guidelines.

Sputum Microbiome

Sputum processing for microbiological analysis

Frozen sputum samples were thawed and any sputum plugs were separated from any saliva like material for analysis. For pre-lysis of sputum plugs transfer ~100mg of sputum plugs to a sterile Eppendorf tube and mixed with an equal volume of 10% dithiothreitol (DTT, Sputolysin®, Calbiochem, CA, USA). Each sample was mixed by vigorous vortexing and incubated at room temperature (R^oT) for 30 minutes on a thermo-shaker at 2000 RMP. Next add 200 µl lysis buffer (5 mg/mL lysozyme in BLB [Roche Bacteria Lysis Buffer]), vortex thoroughly and incubate for 30 minutes at 37°C in an orbital thermo-shaker at 2000 RMP. Transfer the total volume to a glass bead tubes (matrix A) and homogenize on the FastPrep®-24 instrument (MP Biomedical, CA, USA) at speed setting 6.0 for 40 seconds. Remove the sample tubes from the FastPrep®-24 instrument and centrifuge at 13,000 x g for 1 minute. To the homogenized sample add 32 µl of proteinase K (20 mg/mL, Qiagen, Hilden, Germany) and mix thoroughly by vortexing. Incubate at 65°C for 10 minutes on a heated thermo-shaker at 1500 RMP. Next add 150µl of nuclease free water, place the tube in the FastPrep®-24 instrument (MP Biomedical, CA, USA) and homogenize at speed setting 6.0 for 40 seconds. Incubate the homogenized sample at 95°C for 10 minutes on a heated thermo-shaker at 1000 RMP. Finally, centrifuge at 10,000 x g for 10 minutes at 4°C and transfer 200 µl to a sterile Eppendorf tube for storing at -80°C until further use.

Extraction of gDNA from sputum samples

Pre-lysed samples were extracted on the Roche MagNA Pure extraction system (Roche Diagnostics Limited, West Sussex, UK) according to manufacturer's instructions.

Library preparation for the Illumina MiSeq amplicon sequencing

Sample processing and library generation was performed as previously described by Lundberg et al. (1) Briefly, the library generation was as follows: PCR 1: Pre-amplification of 16S rRNA marker gene region is necessary for potentially low biomass template in order to carry enough tagged amplicon through to the final indexing-amplification steps. Perform PCR using ~200 ng of gDNA from each sample. Using non-modified primers targeting positions 515F and 806R within the V4 region of the 16S rRNA marker gene prepare a mastermix solution [5 μ l 5x Phusion Hifi Buffer, 0.5 μ l (10 mM) dNTP, 1 μ l (10 μ M) V4 primer mix; 0.25 μ l Phusion HS II polymerase and make to 25 μ l per reaction using DEPC water] and amplify using the following condition: 98°C for 30 seconds (x1) \rightarrow 98°C for 10 seconds + 52°C for 30 seconds + 72°C for 20 seconds (10 cycles) \rightarrow 72°C for 5 minutes \rightarrow hold at 4°C for ∞ . Next clean-up the PCR products from PCR 1 using AxyPrep Mag PCR Clean-up kit as follows; vortex magnetic beads well before use to resuspend any magnetic beads that may have settled. Aliquot 15 μ l of Axygen beads to 10 μ l of PCR product into a sterile 96 well plate. Mix well by repeated pipetting and incubate at R $^{\circ}$ T for 5 minutes. Place the reaction plate onto the IMAG magnetic separation device and wait until the liquid turns clear. Remove the clear liquid from the plate and discard. Next add 180 μ l of 70% EtOH to each well of the reaction plate and incubate for 30 seconds at R $^{\circ}$ T. Remove the 70% EtOH from each well and discard. Repeat the previous step once. Air dry the beads at R $^{\circ}$ T for no more than 5 minutes and be careful not to over dry the magnetic beads as this will cause the beads to crack and lead to decreased elution efficiency. Ensure that all the ethanol has been removed from each well. Add 11 μ l of molecular grade H₂O to each well. Remove reaction plate from the IMAG separation device and mix well by gentle vortexing. Place the reaction plate onto the IMAG separation device for 1 minute to separate the beads from the solution. Transfer 10 μ l of the cleaned up PCR product to a sterile 96 well plate for the next PCR step. PCR 2: Reverse Tagging Step using the cleaned product from PCR 1 using equimolar mixture of the reverse frame-shift (FS) primers 808R_f1, 808R_f2, 808R_f3, 808R_f4, 808R_f5, 808R_f6). Primers are combined into a working stock of 0.5 μ M. Perform 1 cycle PCR using 10 μ l of product from PCR 1. Prepare a mastermix solution [5 μ l 5x Phusion Hifi Buffer, 0.5 μ l (10 mM) dNTP, 2 μ l (0.5 μ M, Reverse_MT_tag Primer mix); 0.25 μ l Phusion HS II polymerase and 7.25 μ l DEPC water] and amplify using the following condition: 98°C for 60 seconds (x1) \rightarrow 98°C for 10 seconds + 50°C for 30 seconds + 72°C for 60 seconds (1 cycle) \rightarrow hold at 4°C for ∞ . Next clean-up the PCR products from PCR 1 using AxyPrep Mag PCR Clean-up kit as follows; vortex magnetic beads well before use to resuspend any magnetic beads that may have settled. Aliquot 15 μ l of Axygen beads to 10 μ l of PCR product into a sterile 96 well plate. Mix well by repeated pipetting and incubate at R $^{\circ}$ T for 5 minutes. Place the

reaction plate onto the IMAG magnetic separation device and wait until the liquid goes clear. Remove the clear liquid from the plate and discard. Next add 180 µl of 70% EtOH to each well of the reaction plate and incubate for 30 seconds at R^oT. Remove the 70% EtOH from each well and discard. Repeat the previous step once. Air dry the beads at R^oT for no more than 5 minutes and be careful not to over dry the magnetic beads as this will cause the beads to crack and lead to decreased elution efficiency. Ensure that all the ethanol has been removed from each well. Add 11 µl of DECP water to each well. Remove reaction plate from the IMAG separation device and mix well by gentle vortexing. Place the reaction plate onto the IMAG separation device for 1 minute to separate the beads from the solution. Transfer 10 µl of the cleaned up PCR product to a sterile 96 well plate for the next PCR step. PCR 3: Forward-Tagging Step using the cleaned product from PCR 2 using equimolar mixture of the forward frame-shift (FS) primers 515F_f1, 515F_f2, 515F_f3, 515F_f4, 515F_f5, 515F_f6). Primers are combined into a working stock of 0.5 µM. Perform 1 cycle PCR using 10 µl of product from PCR 2. Prepare a mastermix solution [5 µl 5x Phusion Hifi Buffer, 0.5 µl (10 mM) dNTP, 2 µl (0.5 µM, Reverse_MT_tag Primer mix); 0.25 µl Phusion HS II polymerase and 7.25 µl DEPC water] and amplify using the following condition: 98°C for 60 seconds (x1) → 98°C for 10 seconds + 50°C for 30 seconds + 72°C for 60 seconds (1 cycle) → hold at 4°C for ∞. Next clean-up the PCR products from PCR 3 using AxyPrep Mag PCR Clean-up kit as follows; vortex magnetic beads well before use to resuspend any magnetic beads that may have settled. Aliquot 17.5 µl of Axygen beads to 10 µl of PCR product into a sterile 96 well plate. Mix well and incubate at R^oT for 5 minutes. Next place the reaction plate onto the IMAG magnetic separation device and wait until the liquid goes clear. Remove the clear liquid from the plate and discard. Add 180 µl of 70% EtOH to each well of the reaction plate and incubate for 30 seconds at R^oT. Remove the 70% EtOH from each well and discard. Repeat previous step once. Air dry the beads at R^oT for no more than 5 minutes, be careful not to over dry the magnetic beads as this will cause the beads to crack and lead to decreased elution efficiency. Ensure that all the ethanol has been removed from each well. Add 16 µl of DEPC water to each well and remove the reaction plate from the IMAG magnetic separation device and mix well to resuspend the magnetic beads. Next place the reaction plate onto the IMAG separation device for 1 minute to separate the beads from the solution. Transfer 15 µl of the cleaned up PCR product to a sterile 96 well plate for the next PCR step. PCR 4: Nextera-Adapter/Indexing Amplification step by performing a 34 cycle PCR, targeting the V4 region of the 16S rRNA marker gene, using 15 µl of the cleaned reverse and forward tagged product from step PCR 3. Each reaction will have the same forward primers and a unique reverse primer which acts as the index (barcode) for each sample. The forward and reverse primers are typically diluted to a working stock of 5 µM

and can be added separately to each reaction (the forward primer is universal and could be added to any master-mixes instead), or the forward primer can be added to each reverse primer in a working stock in a plate for further use. Prepare a mastermix solution [10 µl 5x Phusion Hifi Buffer, 1µl (10 mM) dNTP, 2.5 µl forward primer (SEQ_V4_F; AATGATACGGCGACCACCGAGATCTACACGCCTCCCTCGCGCCATCAGAGATGTG); 2.5µl reverse primer (INDEX_R_bc1 to bc96; CAAGCAGAAGACGGCATAACGAGAT XXXXXXXX GTGACTGGAGTTCAGACGTGTGCTC); 0.5 µl Phusion HS II polymerase and 7.25 µl DEPC water] and amplify using the following condition: 98°C for 30 seconds (x1) → 98°C for 10 seconds + 63°C for 30 seconds + 72°C for 30 seconds (34 cycle) → hold at 4°C for ∞. Next run 5 µl of each reaction on a 1% agarose gel to visually confirm presence of products (~453bp). Clean the PCR products from step PCR 4 with AxyPrep Mag PCR Clean-up kit as follows; vortex magnetic beads well before use to resuspend any magnetic beads that may have settled. Aliquot 35 µl of Axygen beads and the entire PCR product into a sterile 96 well plate and mix well and incubate at R°T for 5 minutes. Next place the reaction plate onto the IMAG magnetic separation device and wait until the liquid goes clear. Remove the clear liquid from the plate and discard. Add 180 µl of 70% EtOH to each well of the reaction plate and incubate for 30 seconds at R°T. Remove the 70% EtOH from each well and discard. Repeat the previous step once. Air dry the beads at R°T for no more than 5 minutes, avoiding to not over drying the magnetic beads as this will cause the beads to crack and lead to decreased elution efficiency. Next add 50 µl of DEPC water to each well and remove reaction plate from the IMAG magnetic separation device and mix well. Place the reaction plate back onto the IMAG magnetic separation device for 1 minute to separate the beads from the solution. Transfer all of the cleaned up PCR product to a sterile 96 well plate. Next quantify products using Quant-iT™ PicoGreen® dsDNA Assay kit (Life Technologies, Paisley, UK) in a 96 well plate using 2 µl of cleaned product. Pool equimolar amounts from each sample adding no more than 20 µl of each reaction to the final pool. Typically, only reactions that failed will need to be added at this volume (the pool will not be equimolar for them). Gel purify the pool by running it on a 1% agarose gel and gel extracting the correct size band (~453bp) using the QIAEX II kit (Qiagen, Manchester,UK) according to manufactures instructions, removing as much of the excess agarose gel as possible. The final sample pool was quantified in triplicate using the Quant-iT™ PicoGreen® dsDNA Assay kit (Life Technologies, Paisley, UK) and the concentration converted to nM (minimum 4 nM required). Samples were stored at -20°C/-80°C until submission for Illumina MiSeq sequencing.

Molecular detection - Illumina MiSeq data processing

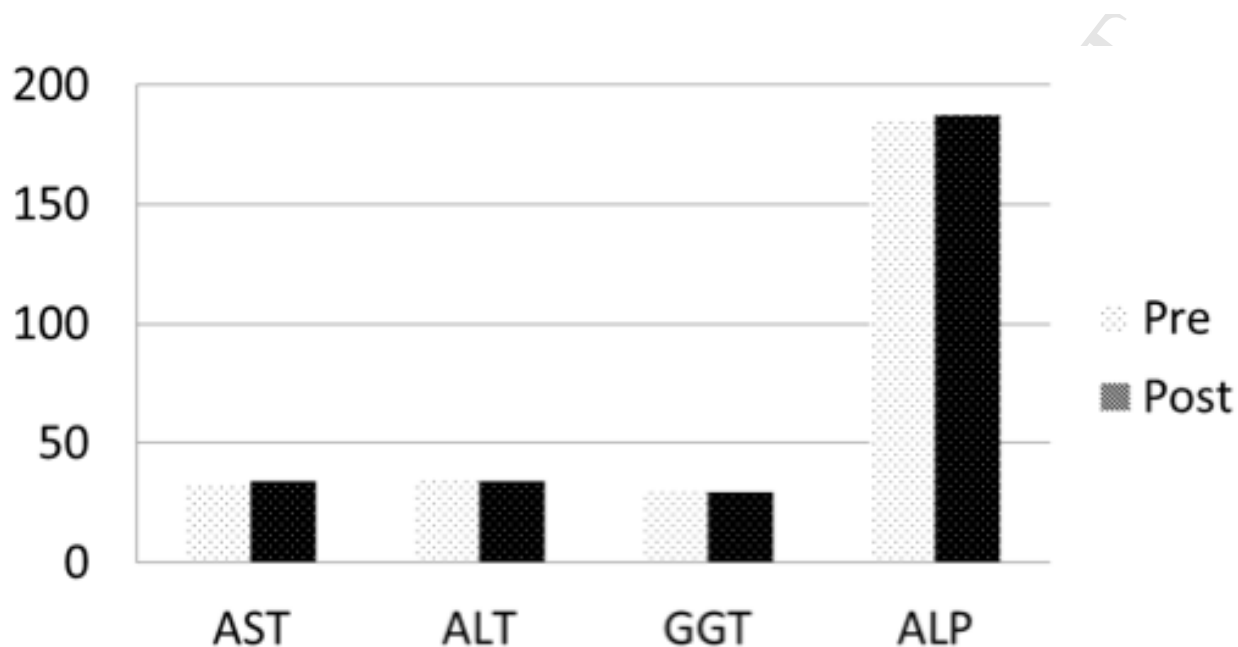
Paired-end Illumina MiSeq sequences were processed using QIIME (Quantitative Insights into Microbial Ecology; version 1.8.0), (2) by joining the corresponding paired-end reads, removing the Illumina adapters and barcode sequences. We removed sequences with length less than 200 and longer than 400 nucleotides, as well as sequences with an average quality score (Phred score) of $<Q30$. Sequences lacking an exact match to a 5' primer were also removed from the dataset along with sequences that contained any mismatches in the barcode sequence. Following this initial processing step, we removed potential chimeric sequences from downstream processing through the implementation of Chimera Slayer. (3) Sequences were then clustered into their representative OTUs based on the 97% sequence identity using the UCLUST algorithm, (4) aligned against full length 16S rRNA marker gene sequences from the Greengenes reference alignment (version 13.8) by PyNAST (5) and assigned their taxonomic identities according to the Ribosomal Database Project Classifier Tool (v 2.2) (6) using an open reference OTU picking as implemented within QIIME. A number of taxa were detected in the background of the negative control, however this community lacked a strong dominance by any single taxon. Furthermore, singletons (i.e. taxa represented by a single read over all the samples) and OTUs representing potential human sequences, Archaea, Cyanobacteria, unassigned OTUs and those found in the background of the negative control were filtered out and treated as contaminating sequences prior to all downstream analysis. The resulting dataset was then converted to a final quality filtered OTU table and presented either normalised absolute counts or relative abundance.

REFERENCES

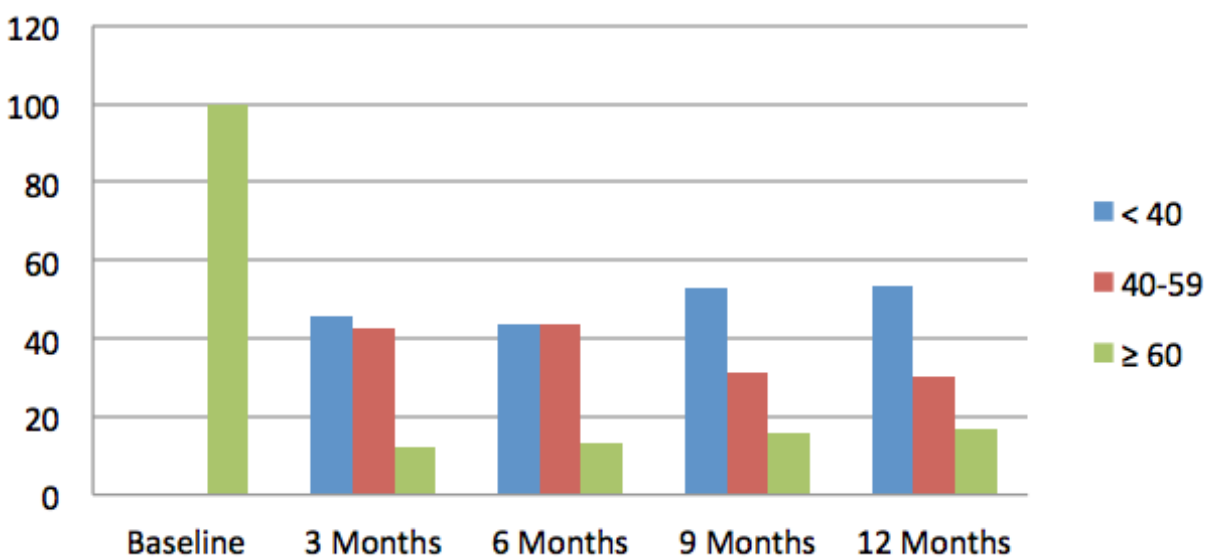
1. Lundberg DS, Yourstone S, Mieczkowski P, Jones CD, Dangi JL. Practical innovations for high-throughput amplicon sequencing. *Nat Meth* 2013;10:999-1002.
2. Caporaso JG, Kuczynski J, Stombaugh J, Bittinger K, Bushman FD, Costello EK, Fierer N, Pena AG, Goodrich JK, Gordon JI. Qiime allows analysis of high-throughput community sequencing data. *Nat Methods* 2010;7:335-336.
3. Haas BJ, Gevers D, Earl AM, Feldgarden M, Ward DV, Giannoukos G, Ciulla D, Tabbaa D, Highlander SK, Sodergren E, Methé B, DeSantis TZ, Consortium THM, Petrosino JF, Knight R, Birren BW. Chimeric 16s rRNA sequence formation and detection in sanger and 454-pyrosequenced PCR amplicons. *Genome Res* 2011;21:494-504.
4. Edgar RC, Haas BJ, Clemente JC, Quince C, Knight R. Uchime improves sensitivity and speed of chimera detection. *Bioinformatics* 2011;27:2194-2200.
5. Caporaso JG, Bittinger K, Bushman FD, DeSantis TZ, Andersen GL, Knight R. Pynast: A flexible tool for aligning sequences to a template alignment. *Bioinformatics* 2010;26:266-267.
6. Wang Q, Garrity GM, Tiedje JM, Cole JR. Naive bayesian classifier for rapid assignment of rRNA sequences into the new bacterial taxonomy. *Appl Environ Microbiol* 2007;73:5261-5267.

Supplemental Results

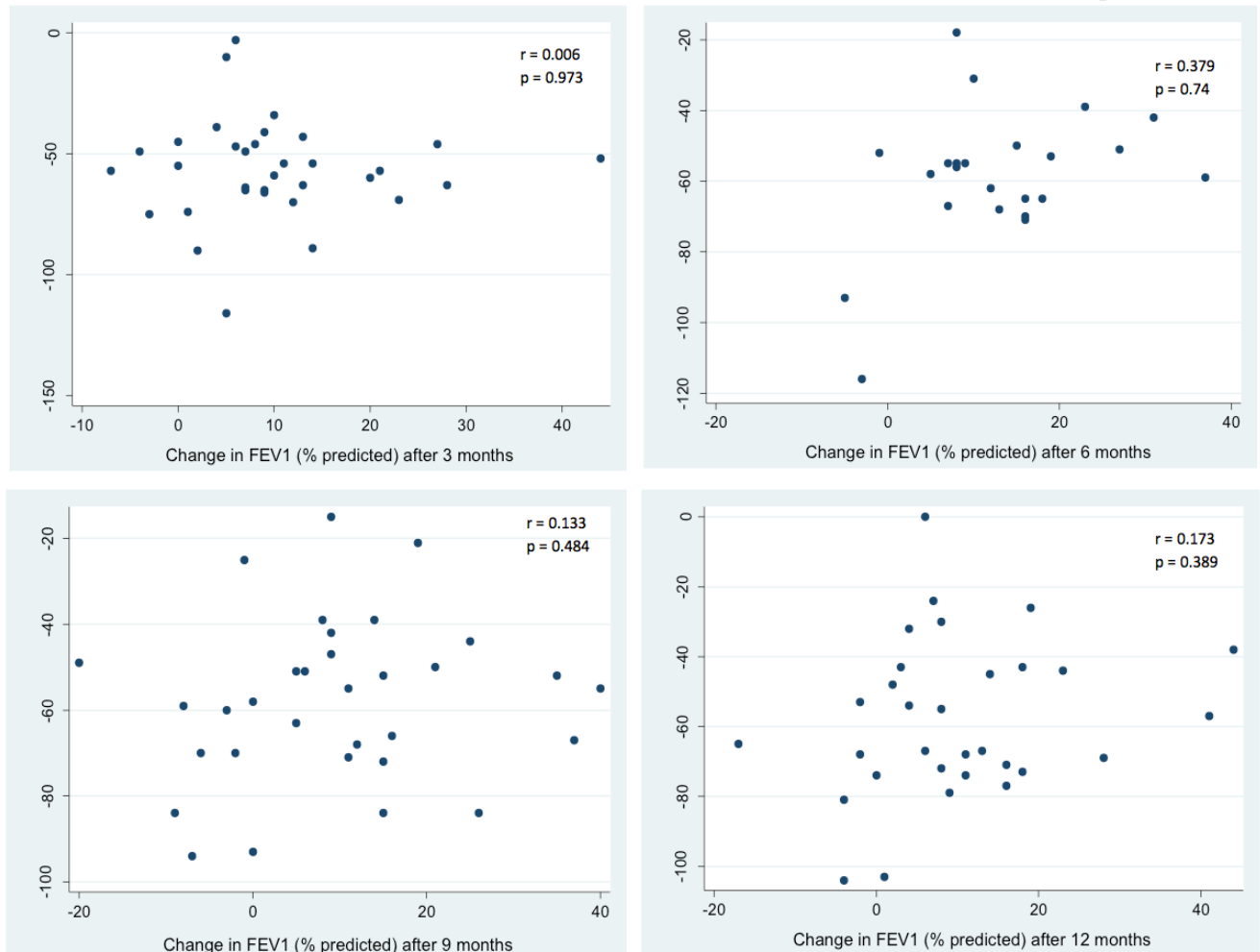
e-Figure 3. Mean Liver Function Test before and after treatment.



e-Figure 4. Percentage of patients in each sweat chloride category.



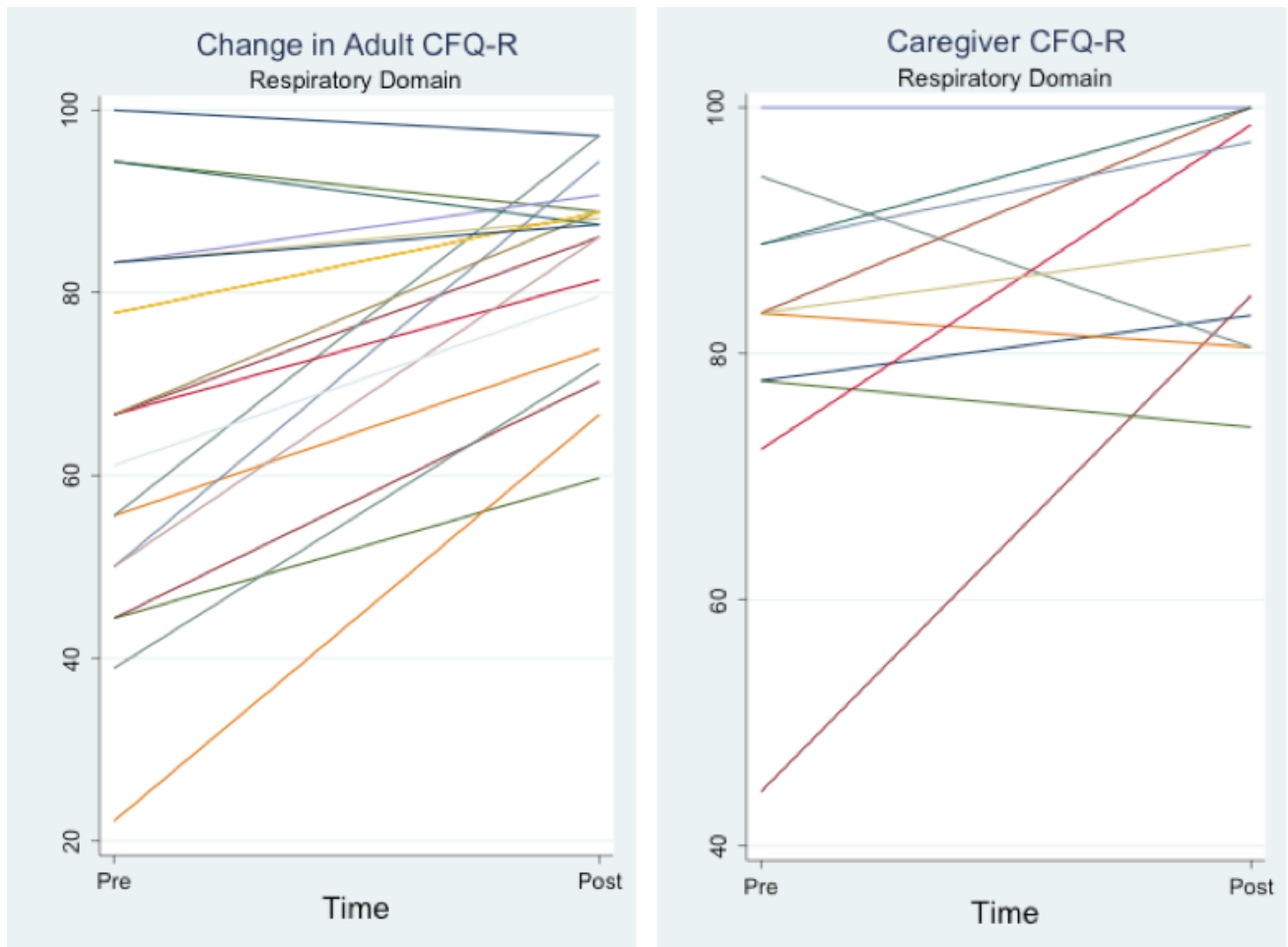
e-Figure 5. Relationship between change in FEV1 (% predicted) and change in sweat chloride (mmol/l).



Change in Adult and Paediatric CFQ-R after commencement of ivacaftor

e-Table 1 Adult CFQ-R (N = 20)

CFQ-R Domain	Mean baseline score (SD)	Mean change (SD)	P value
Eating	92.78 (15.8)	2.036 (8.7)	0.312
Physical	86 (17.6)	4.35 (12.6)	0.139
Vitality	66.25 (15.87)	5.5 (13.5)	0.082
Emotion	79.76 (15.6)	2.4 (7.88)	0.188
Treatment burden	67.24 (18.56)	5.6 (14.9)	0.109
Health perception	74.46 (19.78)	6.1 (18.7)	0.161
Social	78.33 (14.95)	0.88 (12.78)	0.761
Body Image	69.46 (25.21)	8.8 (22.17)	0.092
Role	86.26 (18.2)	1.66 (8.66)	0.402
Weight	58.34 (37.27)	22.63 (31.22)	0.004
Digestive	86.12 (16.69)	3.06 (10.78)	0.22

e-Figure 6. Change in CFQ-R respiratory domain.

e-Table 2 Parent/care-giver CFQ-R (N = 11)			
CFQ-R Domain	Mean baseline score (SD)	Mean change (SD)	P value
Physical	94.96 (5.6)	1.74 (8.42)	0.489
Emotion	85.5 (12.3)	1.26 (12.79)	0.739
Vitality	73.3 (17.75)	1.11 (10.67)	0.725
School	78.73 (17.36)	2.38 (13.3)	0.548
Eating	86.11 (18.57)	-0.236 (19.26)	0.967
Body Image	75.9 (28.76)	13.73 (18.65)	0.027
Treatment Burden	62.97 (21.38)	-2.0 (17.5)	0.7
Health perception	84.28 (12.9)	-0.7 (18.69)	0.899
Digestive	80.58 (16.48)	7.7 (15.5)	0.113
Weight	63.89 (33.22)	21.76 (33)	0.043